Sectioned images and surface models of a cadaver head with reference to botulinum neurotoxin injection

D.S. Shin[1], Y.J. Shim[2], B.C. Kim[1]

[1]Department of Oral and Maxillofacial Surgery, Daejeon Dental Hospital, Wonkwang University College of Dentistry, Daejeon, Republic of Korea
[2]Department of Oral Medicine, Daejeon Dental Hospital, Wonkwang University College of Dentistry, Daejeon, Republic of Korea

Background: The aim of this study is to elucidate the anatomical considerations with reference to botulinum neurotoxin type A (BTX) injection, on sectioned images and surface models, using Visible Korean. These can be used for medical education and clinical training in the field of facial surgery.
Materials and methods: Serially sectioned images of the head were obtained from a cadaver. Significant anatomic structures in the sectioned images were outlined and assembled to create a surface model.
Results: The PDF file (27.8 MB) of the stacked models can be accessed for free. The file can also be obtained from the authors by email. Using this file, important anatomical structures associated with the BTX injection can be investigated in the sectioned images. All surface models and stereoscopic structures related with the BTX injection are described in real time.
Conclusions: We hope that these state-of-the-art sectioned images, outlined images, and surface models will assist students and trainees in acquiring a better understanding of the anatomy associated with the BTX injection. (Folia Morphol 2018; 77, 3: 564–569)

Key words: cross-sectional anatomy, three-dimensional imaging, botulinum toxins

INTRODUCTION

Injection of botulinum neurotoxin type A (BTX) as a nonsurgical therapy of the facial muscle is generally considered to be a safer and more reliable choice than traditional surgical treatment [20]. However, some side effects have been described, such as muscle weakness, swelling, headache, bruising, xerostomia, and abnormal facial expressions [6]. To avoid such complications, much clinical experience and anatomical knowledge is needed. Of particular importance to medical students and unskilled practitioners is the knowledge of the stereoscopic anatomy of facial muscles, blood vessels, and nerves. Therefore, a better understanding of the anatomy related with the face will make BTX safer and more widely available.

Currently, coloured cross-sectional images at a resolution higher than that provided by computed tomography or magnetic resonance imaging are useful to make stereoscopic images that are helpful for BTX injection. In a previous study, we constructed Vis-
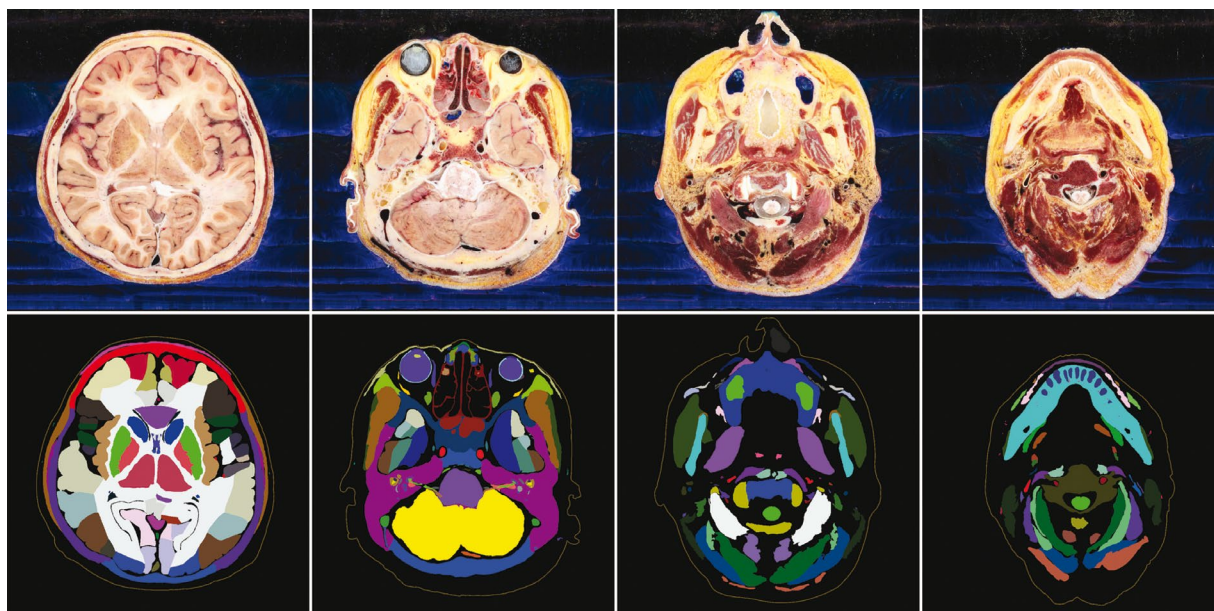
Figure 1. Sectioned and colour-coded images of the head.

ible Korean images from thin-slice (0.2 mm intervals) cross-sectional human datasets that were coloured similar to the in vivo structures [3, 4, 17]. In addition, we made sectioned images and surface models of a cadaver head [15, 16]. In another study, we described software that is accessible to untrained individuals for searching sectional images by anatomic name [14]. These surface models were developed as a portable document format (PDF) file using the software package Adobe Acrobat Pro Extended Version 9 (Adobe Systems, Inc., San Jose, CA, USA) [14].

To date, accumulated data have not effectively been able to describe the BTX injection. Therefore, in this study, we made sectioned images and surface models of the head with reference to the BTX injection, for use in medical education and clinical training in the field of facial surgery. The data will be accessible to facial surgeons and provide a better understanding of the anatomy associated with the BTX injection, ultimately improving outcomes of treatment. Thorough anatomical knowledge maximises therapeutic reliability and prevents doctors from encountering complications. Moreover, the BTX injection can be experienced virtually, using the PDF file described in this study.

MATERIALS AND METHODS
Outlining of the images
Progressive and advanced outlining techniques have been described previously [3, 4, 8, 17, 18].

In those studies, sectioned and outlined images of a male cadaver (0.2 mm intervals; 0.2 mm pixels; 24 bit colour depth; resolution, 3.040 × 2.008; tagged image file format [TIFF]) were made [15, 16, 19]. Only images of the head that were related with BTX were selected for this study.

Additionally, we manually created outlined images of structures associated with BTX injection, such as the facial muscle, using Mimics software (Materialise, Inc., Leuven, Belgium) at 1 mm intervals with a 0.2 mm pixel size (Fig. 1) [4, 15, 16]. The outlines of each structure were filled with a specific colour, either semi-automatically or manually (Fig. 1) [3, 4, 17, 18].

Reconstruction of surface models
As previously noted, surface models of the head were made [4, 16]. Additional surface models specific to the BTX injection were constructed in this study. Outlined images were also surface-reconstructed to enable their application in facial procedures.

In total, 157 structures were subjected to surface reconstruction (Table 1) using Mimics software as described previously [17, 18]. The models were then classified and saved as stereolithography files and subsequently accessed using Maya software.

Virtual injection of the BTX
The reconstructed surface models were systematically colourised to distinguish the combined structures on Maya (Table 1). The skins were semi-transparent to

Table 1. 157 structures, categorised according to the systems and subsequent groups

Skin (47)		right half of skin, left half of skin
	Creases (19)	feet of crow skin creases, baggy lower eyelid skin c., blepharochalasis
		skin c., bunny lines skin c., festoon skin c., glabellar frown line skin c., glabellar transverse line skin c., horizontal forehead lines skin c., horizontal upper lip line skin c., jowl skin c., labiomandibular fold skin c., marionette line skin c., mentolabial c. skin c., midcheek furrow skin c., nasojugal groove skin c., nasola-bial fold skin c., palpebromalar groove skin c., preauricular lines skin c., tear trough skin c.
	Surface landmarks (22)	metopion, glabella, sellion, rhinion, subnasale, stomion, mid lower lip point, pogonion, gnathion, frontal eminence, eurion, interciliary point located on infraorbital notch, lateral orbital rim at the level of lateral canthus, zygomatic porint lacated on outer orbital region, zygion, alare, midpoint of nasolateral fold between alare and cheilion, gonion, cupid blow's peak, cheilion, lower lip points, lateral chin point located 2 cm to pogonion
	Lip (4)	vermillion border, lip, oral commissure, philtrum
Ligament (7)		mandibular retaining lig, zygomatic cutaneous lig, zygomatic lig, orbital retaining lig, lateral orbital thickening, masseteric cutaneous lig, superior temporal septum
Anatomical layer of face (1)		skin thickness
Bone (1)		bone
Muscle (31)		frontalis m., procerus m., orbicularis oculi m.*, corrugator supercilii m.*, depressor supercilii m.*, orbicularis oris m., depressor anguli oris m.*, risorius m.*, zygomaticus major m.*, zygomaticus minor m.*, levator labii superioris m.*, levator labii superioris alaeque nasi m.*, depressor labii inferioris m.*, modiolus m., mentalis m.*, masseter m.*, temporalis m.*, platysma
Artery (10)		dorsal nasal a., inferior labial a., lateral nasal a., nasal septal branch, superior labial a., supraorbital a., supratrochlear a., inferior a. lar branch, facial a., columellar a.
Vein (10)		angular v., inferior labial v., inferior palpebral v., intercanthal v., lateral nasal v., sentinel v., superior palpebral v., supraorbital v., supratrochlear v., facial v.
Nerve (10)		auriculotemporal n., buccal n., external nasal branch of ophthalmic n., infraorbital n., infratrochlear n., mental n., supraorbital n., supratrochlear n., zygomaticofacial n., zygomaticotemporal n.
Gland (2)		submandibular gland, parotid gland
Fat compartments (6)		jowl fat comp., lateral malar fat comp., medial malar fat comp.,
		temporal fat comp., nasolabial fat comp., infraorbital fat comp.
Injection points of the botulium toxin (19)		botulinum rebalancing, crow s feet, infraorbital wrinkles, horizontal forehead lines, glabellar frown lines A standard form for Asian, glabellar frown lines B severe form, bunny lines, plunged tip of nose, gummy smile, nasolabial fold, asymmetric smile, string lip, drooping of the mouth corner, cobble stone chin, masseter hypertrophy, temporalis hypertrophy, platysmal band, hypertrophy of parotid gland, hypertrophy of submandibular gland
Anatomical images (13)		

(Number of structures); *Bilateral structures; m. — muscle, a. — artery, v. — vein, n. — nerve, c — creases, comp. — compartment, lig. — ligament

allow easy identification of internal structures (Fig. 2). The surface models were modified as required by an anatomist and a maxillofacial surgeon [17, 18]. After painting, virtual injection of the BTX was performed (Fig. 2). The detailed procedure is described in the 'Results' section.

PDF file for the surface models

Stereolithography files were categorised by structure, and the surface models were anatomically arranged using Deep Exploration Standard (Right Hemisphere, San Ramon, CA, USA) [17, 18]. The stereolithography files were constructed and saved under the filename botulinum.pdf using four-dimensional reviewer, a software package accompanying Acrobat 9.0 Pro Extended (Adobe Systems, Inc., San Jose, CA, USA) [17, 18]. Since the PDF file was accessed using Adobe Reader, the individual anatomical names and virtual injection of the BTX were described in the model tree window. In Acrobat, we constructed bookmarks for the BTX injection and the names of related structures (Fig. 3).
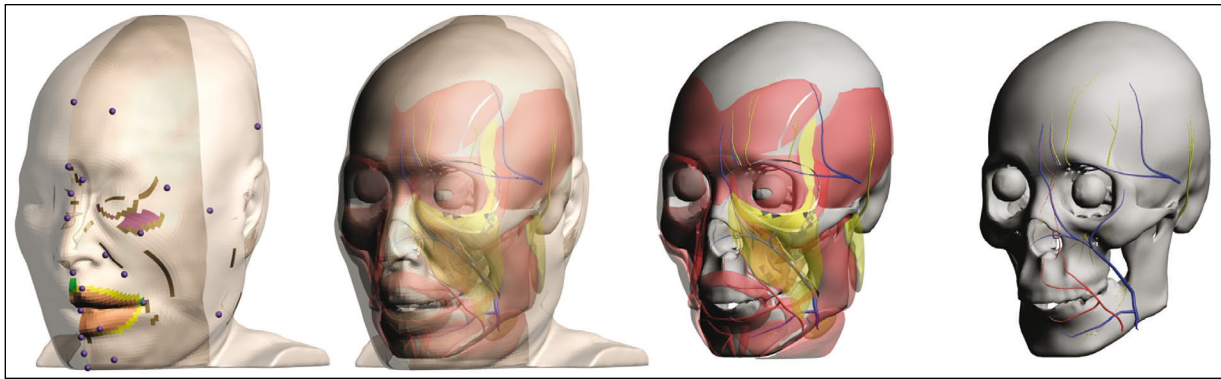
Figure 2. Surface models of the skins are coloured semi-transparent to reveal the inner anatomical structures.
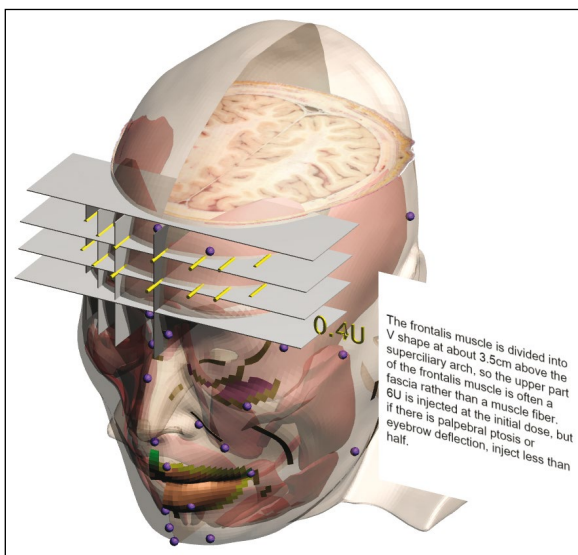

Figure 3. A PDF file with reference to botulinum neurotoxin injection. Sectioned images and stereoscopic surface models of the head can be simultaneously or individually investigated.
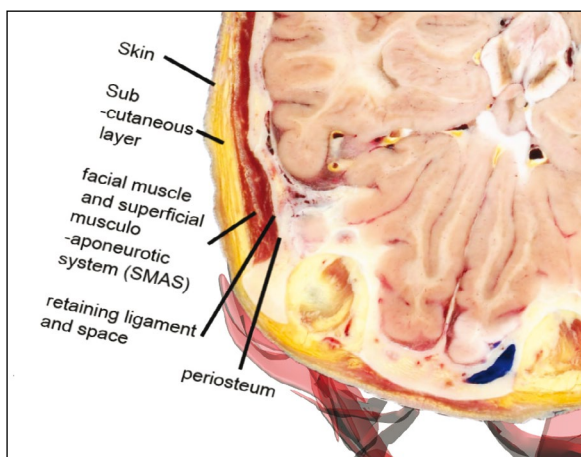

Figure 4. A PDF file showing anatomical layers with reference to botulinum neurotoxin injection.

RESULTS

The PDF file (27.8 MB) is accessible for free (Supplementary Figure 1 — see journal website). It can also be obtained from the authors by email. In the sectioned images, structures related with BTX injection can be investigated and assessed as anatomically appropriate.

Additionally, the surface models and stereoscopic structures associated with the BTX injection were described in real time. Significant anatomic structures can easily be confirmed in the sectional images and stereoscopic aspects of the PDF file, as described in the following examples.

In the sectioned images, the user can identify the face layer such as the superficial muscular aponeurotic system. The position, depth, and diameter of the artery, vein, and nerve that should be noted in the BTX injection can also be confirmed (Fig. 4). With this knowledge, the user can know where and to what depth BTX should be injected.

On the stereoscopic surface models, the user can see where the main artery, vein, and nerve of the face run. Additionally, the main wrinkles of the face, where the muscles run, and fat distribution can all be confirmed (Fig. 3). Moreover, bookmarks in the pdf file can be used to observe where and how much BTX should be injected (Fig. 3). Thus, the user can use the surface models to take the appropriate precautions to avoid complications while injecting BTX. These images can assist the user in becoming accustomed to the BTX injection.

DISCUSSION

Botulinum neurotoxin type A injection is a commonly used non-invasive procedure for the aesthetic treatment of facial features. To successfully perform the BTX injection, it is crucial to understand the stereoscopic anatomy of the face [2, 5, 7, 9–12, 21–23].

Therefore, it is vital that untrained students, or trainees in particular, should understand anatomy prior to clinical practice. To this end, we conducted the present study.

The PDF file described in this study provides scientific data that can be manipulated offline, unlike other surface models such as Visiblebody or Zygotebody [1, 13]. Importantly, the surface models in this study were created on the basis of scientific data. The models were made by outlining structures in serially sectioned images, stacking these outlines, and connecting the outlines using a polygon-based surface reconstruction method [3, 4, 17, 18]. The resultant models are thorough and differ from currently accessible surface models, which are manually created by artists with anatomical knowledge. The surface models produced by us also provide equivalent sectional images (Fig. 4). Users can download the pdf file of this study and check the main anatomical structures for reference before performing the BTX procedure. The PDF file is also useful when describing details to a patient who is undergoing the procedure.

CONCLUSIONS

In conclusion, we expect that the surface models and sectioned images described in this study will enable a thorough understanding of the facial anatomy associated with BTX injection, ensuring better results of facial aesthetic procedures using BTX. Importantly, the results of this study will benefit students and trainees in facial surgery and help them in thoroughly comprehending the principles underlying the use of the BTX.

Acknowledgements

REFERENCES

1. http://www.zygotebody.com.
2. Choi YJ, Kim JS, Gil YC, et al. Anatomical considerations regarding the location and boundary of the depressor anguli oris muscle with reference to botulinum toxin injection. Plast Reconstr Surg. 2014; 134(5): 917–921, doi: 10.1097/PRS.0000000000000589, indexed in Pubmed: 25347627.
3. Kim BC, Chung MS, Kim HJ, et al. Sectioned images and surface models of a cadaver for understanding the deep circumflex iliac artery flap. J Craniofac Surg. 2014; 25(2): 626–629, doi: 10.1097/SCS.0000000000000645, indexed in Pubmed: 24621709.
4. Kim BC, Chung MS, Park HS, et al. Accessible and informative sectioned images and surface models of the maxillo-facial area for orthognathic surgery. Folia Morphol. 2015; 74(3): 346–351, doi: 10.5603/FM.2015.0052, indexed in Pubmed: 26339816.
5. Kim HS, Pae C, Bae JH, et al. An anatomical study of the risorius in Asians and its insertion at the modiolus. Surg Radiol Anat. 2015; 37(2): 147–151, doi: 10.1007/s00276-014-1330-6, indexed in Pubmed: 24969170.
6. Kim JH, Shin JH, Kim ST, et al. Effects of two different units of botulinum toxin type a evaluated by computed tomography and electromyographic measurements of human masseter muscle. Plast Reconstr Surg. 2007; 119(2): 711–717, doi: 10.1097/01.prs.0000239453.67423.99, indexed in Pubmed: 17230111.
7. Kim YS, Choi DY, Gil YC, et al. The anatomical origin and course of the angular artery regarding its clinical implications. Dermatol Surg. 2014; 40(10): 1070–1076, doi: 10.1097/01.DSS.0000452661.61916.b5, indexed in Pubmed: 25207758.
8. Kwon K, Shin DS, Shin BS, et al. Virtual endoscopic and laparoscopic exploration of stomach wall based on a cadaver's sectioned images. J Korean Med Sci. 2015; 30(5): 658–661, doi: 10.3346/jkms.2015.30.5.658, indexed in Pubmed: 25931800.
9. Lee HJ, Kang IW, Won SY, et al. Description of a novel anatomic venous structure in the nasoglabellar area. J Craniofac Surg. 2014; 25(2): 633–635, doi: 10.1097/SCS.0000000000000649, indexed in Pubmed: 24621711.
10. Lee JG, Yang HM, Choi YJ, et al. Facial arterial depth and relationship with the facial musculature layer. Plast Reconstr Surg. 2015; 135(2): 437–444, doi: 10.1097/PRS.0000000000000991, indexed in Pubmed: 25626791.
11. Lee SH, Lee HJ, Kim YS, et al. What is the difference between the inferior labial artery and the horizontal labiomental artery? Surg Radiol Anat. 2015; 37(8): 947–953, doi: 10.1007/s00276-015-1447-2, indexed in Pubmed: 25724940.
12. Lee SH, Lee M, Kim HJ. Anatomy-based image processing analysis of the running pattern of the perioral artery for minimally invasive surgery. Br J Oral Maxillofac Surg. 2014; 52(8): 688–692, doi: 10.1016/j.bjoms.2014.07.098, indexed in Pubmed: 25081954.
13. Liew S, Dart A. Nonsurgical reshaping of the lower face. Aesthet Surg J. 2008; 28(3): 251–257, doi: 10.1016/j.asj.2008.03.003, indexed in Pubmed: 19083534.
14. Shin DS, Chung MS, Park HS, et al. Browsing software of the Visible Korean data used for teaching sectional anatomy. Anat Sci Educ. 2011; 4(6): 327–332, doi: 10.1002/ase.249, indexed in Pubmed: 22065474.
15. Shin DS, Chung MS, Park JS. Systematized methods of surface reconstruction from the serial sectioned images of a cadaver head. J Craniofac Surg. 2012; 23(1): 190–194, doi: 10.1097/SCS.0b013e3182418e87, indexed in Pubmed: 22337405.
16. Shin DS, Jang HG, Park JS, et al. Accessible and informative sectioned images and surface models of a cadaver head. J Craniofac Surg. 2012; 23(4): 1176–1180, doi: 10.1097/SCS.0b013e31825657d8, indexed in Pubmed: 22801119.
17. Shin DS, Kim HJ, Kim BC. Sectioned images and surface models of a cadaver for understanding the dorsalis pedis flap. J Craniofac Surg. 2015; 26(5): 1656–1659, doi: 10.1097/SCS.0000000000001618, indexed in Pubmed: 26079120.

18. Shin DS, Kim HJ, Kim BC. Sectioned images and surface models of a cadaver for understanding the free vascularised anterior rib flap. Folia Morphol. 2017; 76(1): 117–122, doi: 10.5603/FM.a2016.0035, indexed in Pubmed: 27830889.

19. Shin D, Park J, Park H, et al. Outlining of the detailed structures in sectioned images from Visible Korean. Surg Radiol Anat. 2012; 34(3): 235–247, doi: 10.1007/s00276-011-0870-2.

20. von Lindern JJ, Niederhagen B, Appel T, et al. Type A botulinum toxin for the treatment of hypertrophy of the masseter and temporal muscles: an alternative treatment. Plast Reconstr Surg. 2001; 107(2): 327–332, indexed in Pubmed: 11214045.

21. Yang HM, Kim HJ, Hu KS. Anatomic and histological study of great auricular nerve and its clinical implication. J Plast Reconstr Aesthet Surg. 2015; 68(2): 230–236, doi: 10.1016/j.bjps.2014.10.030, indexed in Pubmed: 25465135.

22. Yang HM, Lee JG, Hu KS, et al. New anatomical insights on the course and branching patterns of the facial artery: clinical implications of injectable treatments to the nasolabial fold and nasojugal groove. Plast Reconstr Surg. 2014; 133(5): 1077–1082, doi: 10.1097/PRS.0000000000000099, indexed in Pubmed: 24445874.

23. Yang HM, Won SY, Lee YI, et al. The Sihler staining study of the infraorbital nerve and its clinical complication. J Craniofac Surg. 2014; 25(6): 2209–2213, doi: 10.1097/01.scs.0000436676.43949.19, indexed in Pubmed: 25329852.